Modeling and estimation of the direction-delay power spectrum of the propagation channel

Yin, Xuefeng; Liu, Lingfeng; Pedersen, Troels; Nielsen, Daniel K.; Fleury, Bernard Henri

Published in:
2008 3rd International Symposium on Communications, Control and Signal Processing, Vol 1-3

DOI (link to publication from Publisher):
10.1109/ISCCSP.2008.4537224

Publication date:
2008

Document Version
Publisher's PDF, also known as Version of record

Modeling and Estimation of the Direction-Delay Power Spectrum of the Propagation Channel

Xuefeng Yin [1)], Lingfeng Liu [1), 2)], Troels Pedersen [1)], Daniel K. Nielsen [1)], and Bernard H. Fleury [1), 3)]

[1)] Section Navigation and Communications, Department of Electronic Systems,
Aalborg University, Aalborg, Denmark
[2)] Electromagnetics Microwave Communication, Department of Electricity,
Université Catholique de Louvain, Louvain-la-Neuve, Belgium
[3)] Forschungszentrum Telekommunikation Wien (ftw.), Vienna, Austria

***Abstract*— In this contribution, a multi-variate probability density function (pdf) is derived and used to describe the normalized direction–(i.e. azimuth and elevation)–delay power spectral density of individual dispersed components in the response of the propagation channel. This pdf maximizes the entropy under the constraint that its first and second moments are specified. We use a SAGE algorithm, as an approximation of the maximum-likelihood method, to estimate the parameters of the component direction–delay power spectral densities from measurement data. The experimental results show that the proposed pdf and the SAGE algorithm form altogether an effective tool to characterize direction-delay dispersion in the propagation channel.**

***Index Terms*— Propagation channel, direction–delay power spectrum, SAGE algorithm.**

I. Introduction

Due to the heterogeneity of the propagation environment, the received signal at the receiver (Rx) of a radio communication system can be modelled as the superposition of a number of components originating from waves propagating along specific propagation paths. Each component may be dispersive in delay, direction of departure (DoD), direction of arrival (DoA), Doppler frequency and polarization. Dispersion of individual components in these dimensions significantly influences the performance of communication systems using MIMO (multiple-input multiple-output) techniques [1].

In conventional parametric models for the MIMO wideband propagation channel, such as [2, Chapter 3], [3] and [4], dispersion of individual components is modeled using a cluster of multiple specular components estimated from measurement data. The cluster parameters, such as the nominal direction and direction spread, can be calculated for each cluster from the parameter estimates of the specular components assigned to this cluster. However, as shown in [5], the extracted dispersion parameters (e.g. azimuth) of the specular components do not accurately characterize the true dispersive behavior of the original component when this component is dispersed. This phenomenon limits the reliability of channel models derived based on specular components estimated from measurement data collected in real environments. Therefore, in order to design more realistic channel models we need appropriate parametric models characterizing dispersion of individual components, as well as efficient estimators of the parameters entering these models.

In recent years, various algorithms have been proposed for the estimation of the dispersive characteristics of individual components in the channel response [1], [6], [7], [8]. These algorithms estimate the parameters describing the power spectral density (psd) of individual components. In real environments, a component psd can be irregular due to the heterogenous physical and electromagnetic properties of the scatterers with which the waves generating this component interact. The center of gravity and spreads of a component psd are considered as the characteristic dispersion parameters. The algorithms proposed in these contributions estimate these parameters by approximating the component psd with a certain probability density function (pdf), e.g. in azimuth–of–arrival (AoA) [6], [7], [8] and in AoA and azimuth of departure (AoD) [1]. The values of the parameter estimates obtained by using these algorithms depend on the underlying pdfs. However, no rationale behind the selection of the pdfs is given in these contributions. Furthermore, the performance of these algorithms has not been investigated using measurement data.

In order to obtain accurate estimates of the dispersion parameters, a rationale relying on the maximum-entropy (ME) principle [9] is proposed in [10], [11], [12] for the selection/derivation of the pdfs characterizing component psds. This rationale utilizes the assumptions that each component psd has fixed center of gravity and spreads, and moreover, no information is available for any other properties, such as the exact shape and number of local maxima, of the component psd. The center of gravity and the spreads of a component psd are described by the first and second moments of a pdf. Thus, using the ME principle we derive a pdf which satisfies the constraint of fixed first and second moments, while maximizes the entropy of any other constraint. The estimates of the dispersion parameters obtained by modeling the component psd with this entropy-maximizing pdf provide the "safest" results in the sense that, they are more accurate than the estimates computed using a pdf subject to any constraint that is invalid in real situations. Based on this rationale, a bivariate von-Mises-Fisher pdf and a Fisher-Bingham-5 (FB_5) pdf are derived for

978-1-4244-1688-2/08/$25.00

modeling the component psd in AoA and AoD [10] and in elevation and azimuth [11], [12] respectively. Experimental investigations using measurement data demonstrate that these characterizations are applicable in real environments.

In this contribution, we consider a single-input multiple-output (SIMO) scenario where the propagation channel is dispersive in DoA (i.e. azimuth and elevation of arrival) and delay. We propose to characterize the component DoA–delay psd by a multi-variate pdf. The applicability of this characterization method is evaluated using measurement data. With proper modifications, the characterization method can be used to describe dispersion of individual components in DoD (i.e. azimuth and elevation of departure) and delay in a multiple-input single-output (MISO) scenario.

The organization of this contribution is as follows. In Section II, the signal model for SIMO channel sounding is presented. Section III introduces the derived pdf characterizing the shape of the component DoA–delay psd. In Section IV, the SAGE estimators of the parameters of the psd are briefly described. Section V presents the results from experimental investigations. Finally, concluding remarks are addressed in Section VI.

II. Signal Model and Assumptions

In this section, we introduce the signal model for SIMO channel sounding and state our assumptions on dispersion in DoA and delay in the propagation channel.

A. Signal Model for SIMO Channel Sounding

The channel sounder considered here has a single antenna in the Tx and M antennas in the Rx. We focus on a scenario where the propagation channel is dispersive in delay $\tau \in \mathbb{R}$ and DoA $\mathbf{\Omega}$. Here, $\mathbf{\Omega}$ is defined to be a unit vector with initial point anchored at the origin $\mathcal{O}$ of a coordinate system located in the vicinity of the Rx array. The end point of $\mathbf{\Omega}$ lies on a unit sphere $\mathbb{S}_2$ centered at $\mathcal{O}$ [13]. The DoA $\mathbf{\Omega}$ is uniquely specified by the azimuth of arrival $\phi \in [-\pi, +\pi)$ and the elevation of arrival $\theta \in [0, \pi]$ according to

$$\mathbf{\Omega} = \boldsymbol{e}(\phi, \theta) \doteq \begin{bmatrix} \cos(\phi)\sin(\theta) \\ \sin(\phi)\sin(\theta) \\ \cos(\theta) \end{bmatrix}. \tag{1}$$

Following the nomenclature in [13], in one measurement period the continuous-time (complex baseband representation of the) output signal of the mth Rx antenna reads

$$Y_m(t) = \int_{-\infty}^{+\infty} \int_{\mathbb{S}_2} c_m(\mathbf{\Omega}) u(t-\tau) H(\mathbf{\Omega}, \tau) \mathrm{d}\mathbf{\Omega} \mathrm{d}\tau + W_m(t), \tag{2}$$

where $c_m(\mathbf{\Omega})$ denotes the response of the mth Rx antenna, $u(t)$ represents the transmitted signal, and $H(\mathbf{\Omega}, \tau)$ is referred to as the DoA-delay spread function of the propagation channel. The noise component $W_m(t)$ in (2) is a circularly symmetric, spatially and temporally white complex Gaussian process with spectral height σ_w^2.

In a scenario with D components, $H(\mathbf{\Omega}, \tau)$ can be decomposed as

$$H(\mathbf{\Omega}, \tau) = \sum_{d=1}^{D} H_d(\mathbf{\Omega}, \tau), \tag{3}$$

where the summand $H_d(\mathbf{\Omega}, \tau)$ represents the DoA-delay spread function of the dth component.

Replacing $H(\mathbf{\Omega}, \tau)$ in (2) with the sum in (3), $Y_m(t)$ can be recast as

$$Y_m(t) = \sum_{d=1}^{D} S_{d,m}(t) + W_m(t), \tag{4}$$

where $S_{d,m}(t)$ is the dth component in the received signal, i.e.

$$S_{d,m}(t) = \int_{-\infty}^{+\infty} \int_{\mathbb{S}_2} c_m(\mathbf{\Omega}) u(t-\tau) H_d(\mathbf{\Omega}, \tau) \, \mathrm{d}\mathbf{\Omega} \mathrm{d}\tau. \tag{5}$$

B. Assumptions for the DoA-Delay Spread Functions

We assume that the component spread function $H_d(\mathbf{\Omega}, \tau)$, $d \in \{1, \ldots, D\}$ are uncorrelated complex (zero-mean) orthogonal stochastic measures, i.e.

$$\mathrm{E}[H_d(\mathbf{\Omega}, \tau)^* H_{d'}(\mathbf{\Omega}', \tau')] = P_d(\mathbf{\Omega}, \tau) \delta_{dd'} \delta(\mathbf{\Omega} - \mathbf{\Omega}') \delta(\tau - \tau'), \tag{6}$$

where $(\cdot)^*$ denotes complex conjugation, $\delta_{..}$ and $\delta(\cdot)$ represent the Kronecker delta and the Dirac delta function respectively, while

$$P_d(\mathbf{\Omega}, \tau) = \mathrm{E}[|H_d(\mathbf{\Omega}, \tau)|^2] \tag{7}$$

is the DoA–delay power spectrum of the dth component. Identity (6) implies that the DoA-delay spread functions of different components are uncorrelated.

Invoking (3), (6) and (7), we can easily show that the spread function $H(\mathbf{\Omega}, \tau)$ of the propagation channel is a complex zero-mean orthogonal stochastic measure, i.e.

$$\mathrm{E}[H(\mathbf{\Omega}, \tau)^* H(\mathbf{\Omega}', \tau')] = P(\mathbf{\Omega}, \tau) \delta(\mathbf{\Omega} - \mathbf{\Omega}') \delta(\tau - \tau'), \tag{8}$$

where

$$P(\mathbf{\Omega}, \tau) = \sum_{d=1}^{D} P_d(\mathbf{\Omega}, \tau) \tag{9}$$

is the DoA-delay power spectrum of the propagation channel. The component power spectrum $P_d(\mathbf{\Omega}, \tau)$ can be written as

$$P_d(\mathbf{\Omega}, \tau) = P_d \cdot f_d(\mathbf{\Omega}, \tau), \tag{10}$$

with P_d and $f_d(\mathbf{\Omega}, \tau)$ representing respectively, the total average power and the (normalized) direction–delay power spectral density (psd) of the dth component.

III. The Direction-Delay Power Spectral Density

In this subsection, we use the Maximum Entropy (ME) rationale proposed in [10], [11] to derive a pdf for modeling the component DoA-delay psd $f_d(\mathbf{\Omega}, \tau)$. We make the assumption that each component psd has its fixed center of gravity and spreads in DoA and in delay. These parameters are represented by the first and the second moments of the pdf. The sought pdf maximizes the entropy under the constraint that its first and second moments are specified.

An ME pdf $f_{\mathrm{ME}}(\mathbf{\Omega}, \tau)$ of the direction variable $\mathbf{\Omega}$ and the delay variable τ under the constraint that its first and second moments are specified, has the form [14]

$$f_{\mathrm{ME}}(\mathbf{\Omega}, \tau) \propto \exp\left\{ \begin{bmatrix} \mathbf{\Omega} - \bar{\mathbf{\Omega}} \\ \tau - \bar{\tau} \end{bmatrix}^{\mathrm{T}} \begin{bmatrix} \boldsymbol{A} & \boldsymbol{c} \\ \boldsymbol{c}^{\mathrm{T}} & -b \end{bmatrix} \begin{bmatrix} \mathbf{\Omega} - \bar{\mathbf{\Omega}} \\ \tau - \bar{\tau} \end{bmatrix} \right\}, \quad (11)$$

where $\bar{\mathbf{\Omega}}$ represents the mean direction with azimuth $\bar{\phi}$ and elevation $\bar{\theta}$, i.e. $\bar{\mathbf{\Omega}} = \boldsymbol{e}(\bar{\phi}, \bar{\theta})$, $\bar{\tau}$ denotes the mean delay, $[\cdot]^{\mathrm{T}}$ represents the transpose operation, $\boldsymbol{A} \in \mathbb{R}^{3\times 3}$ describes the spread of $f_{\mathrm{ME}}(\mathbf{\Omega}, \tau)$ in direction, $b \in \mathbb{R}$ determines the concentration of $f_{\mathrm{ME}}(\mathbf{\Omega}, \tau)$ in delay, and $\boldsymbol{c} \in \mathbb{R}^3$ describes the dependence of the spread of $f_{\mathrm{ME}}(\mathbf{\Omega}, \tau)$ in direction and in delay.

The parameters $\boldsymbol{A}$, $\boldsymbol{c}$ and b arising in (11) are all free parameters. We now determine these parameters under the assumption that the conditional pdfs of (11) with respect to delay and direction coincide with the Gaussian pdf and the FB_5 pdf respectively. These two pdfs are selected specifically because they also maximize the entropy with specified first and second moments.

The Gaussian pdf for the variable delay reads

$$f(\tau) \propto \exp\{-b(\tau - \bar{\tau})^2\}. \quad (12)$$

The FB_5 pdf reads [15]

$$f_{\mathrm{FB}_5}(\mathbf{\Omega}) \propto \exp\{\kappa \boldsymbol{\gamma}_1^{\mathrm{T}} \mathbf{\Omega} + \zeta[(\boldsymbol{\gamma}_2^{\mathrm{T}} \mathbf{\Omega})^2 - (\boldsymbol{\gamma}_3^{\mathrm{T}} \mathbf{\Omega})^2]\}, \quad (13)$$

where $\kappa \geq 0$ and $\zeta \in [0, \kappa/2)$ are respectively the concentration parameter and the ovalness parameter of the distribution on the unit sphere $\mathbb{S}_2$, while $\boldsymbol{\gamma}_1$, $\boldsymbol{\gamma}_2$ and $\boldsymbol{\gamma}_3 \in \mathbb{R}^3$ are unit vectors. The matrix $\mathbf{\Gamma} \doteq [\boldsymbol{\gamma}_1, \boldsymbol{\gamma}_2, \boldsymbol{\gamma}_3]$ is uniquely determined by the three angular parameters $\bar{\phi}$, $\bar{\theta}$ and α according to

$$\mathbf{\Gamma} = \begin{bmatrix} \sin(\bar{\theta})\cos(\bar{\phi}) & -\sin(\bar{\phi}) & \cos(\bar{\theta})\cos(\bar{\phi}) \\ \sin(\bar{\theta})\sin(\bar{\phi}) & \cos(\bar{\phi}) & \cos(\bar{\theta})\sin(\bar{\phi}) \\ \cos(\bar{\theta}) & 0 & -\sin(\bar{\theta}) \end{bmatrix} \cdot \begin{bmatrix} 1 & 0 & 0 \\ 0 & \cos(\alpha) & -\sin(\alpha) \\ 0 & \sin(\alpha) & \cos(\alpha) \end{bmatrix}, \quad (14)$$

where $\bar{\theta}$ and $\bar{\phi}$ coincide with respectively the elevation and the azimuth of the mean direction, i.e. the first moment of $f_{\mathrm{FB}_5}(\mathbf{\Omega})$. The angle α describes tilt of the pdf on $\mathbb{S}_2$. An illustrative description of the meanings of $\boldsymbol{\gamma}_1$, $\boldsymbol{\gamma}_2$ and $\boldsymbol{\gamma}_3$ can be found in [15].

Under the assumption that the pdf $f_{\mathrm{ME}}(\mathbf{\Omega}, \tau)$ in (11) has the conditional direction pdf (13) and the conditional delay pdf (12), the sought pdf (11) is calculated to be

$$f_{\mathrm{ME}}(\mathbf{\Omega}, \tau) \propto \exp\{\kappa \bar{\mathbf{\Omega}}^{\mathrm{T}} \mathbf{\Omega} + \mathbf{\Omega}^{\mathrm{T}} \boldsymbol{A}(\tau, \zeta, \alpha, \beta) \mathbf{\Omega} - b(\tau - \bar{\tau})^2 - 2\eta \boldsymbol{g}^{\mathrm{T}} (\mathbf{\Omega} - \bar{\mathbf{\Omega}})(\tau - \bar{\tau})\}. \quad (15)$$

In (15), the matrix $\boldsymbol{A}$ is a function of the delay τ, the ovalness coefficient ζ, as well as the angles α and β that jointly describe how $f_{\mathrm{ME}}(\mathbf{\Omega}, \tau)$ is tilted in the direction–delay space, η describes the dependence between the spread in direction and in delay, and

$$\boldsymbol{g} = \begin{bmatrix} \sin\bar{\phi}\cos\beta - \sin\bar{\theta}\cos\bar{\phi}\sin\beta \\ -\cos\bar{\phi} - \sin\bar{\theta}\sin\bar{\phi}\sin\beta \\ \cos\bar{\theta}\sin\beta \end{bmatrix}.$$

We assume that the component direction–delay psd $f_d(\mathbf{\Omega}, \tau)$ in (10) is well approximated by the pdf in (15), i.e.

$$f_d(\mathbf{\Omega}, \tau) = f_{\mathrm{ME}}(\mathbf{\Omega}, \tau; \boldsymbol{\theta}_d), \quad (16)$$

where $\boldsymbol{\theta}_d$ contains the component-specific parameters

$$\boldsymbol{\theta}_d \doteq [\bar{\mathbf{\Omega}}_d, \bar{\tau}_d, \kappa_d, \zeta_d, \alpha_d, \beta_d, \eta_d, b_d].$$

The center of gravity of $f_d(\mathbf{\Omega}, \tau)$ coincides with $(\bar{\mathbf{\Omega}}_d, \bar{\tau}_d)$, while the shape of $f_d(\mathbf{\Omega}, \tau)$ is determined jointly by the parameters $\kappa_d, \zeta_d, \alpha_d, \beta_d, \eta_d$ and b_d.

The component azimuth-elevation-delay psd $f_d(\phi, \theta, \tau)$ is induced from $f_d(\mathbf{\Omega}, \tau)$ via the mapping $(\phi, \theta, \tau) \mapsto (\mathbf{\Omega}, \tau)$ to be

$$\begin{aligned} f_d(\phi, \theta, \tau) &= \sin(\theta) \cdot f_d(\mathbf{\Omega}, \tau)\big|_{\mathbf{\Omega}=\boldsymbol{e}(\phi,\theta)} \\ &= \sin(\theta) \cdot f_{\mathrm{ME}}(\mathbf{\Omega}, \tau; \boldsymbol{\theta}_d)\big|_{\mathbf{\Omega}=\boldsymbol{e}(\phi,\theta)}. \end{aligned} \quad (17)$$

Here, $\sin(\theta)$ is the Jacobian resulting from the change of variables. Fig. 1 depicts an example of the 3 dB-spread surface

$$\left\{ (\phi, \theta, \tau) : f_d(\phi, \theta, \tau) = \frac{1}{2} f_d(\bar{\phi}, \bar{\theta}, \bar{\tau}) \right\} \quad (18)$$

computed using (17) for the parameter setting reported in this figure.

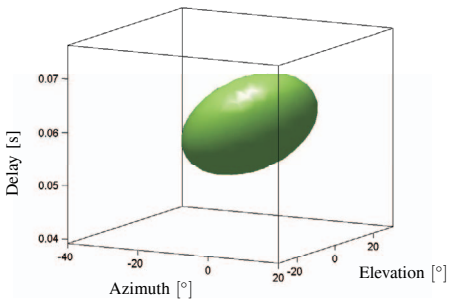

$\bar{\theta}$ [°]	$\bar{\phi}$ [°]	$\bar{\tau}$ [ms]	κ	ζ	α [°]	β [°]	η	b
0	0	58	100	0.01	60	270	1000	40000

Fig. 1. 3 dB-spread surface of the azimuth–elevation–delay psd calculated using (15) with the parameter setting given above.

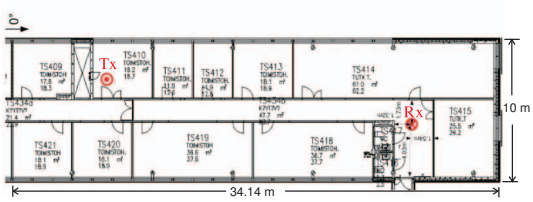

Fig. 2. Map of the investigated propagation environment.

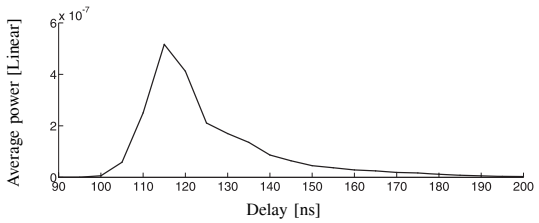

Fig. 3. Estimated delay power spectrum of the received signal.

IV. Parameter Estimator using a SAGE Algorithm

In a scenario with D dispersed components, the unknown parameters in the signal model (2) can be concatenated in the vector

$$\boldsymbol{\theta} \doteq [P_1, \ldots, P_D, \boldsymbol{\theta}_1, \ldots, \boldsymbol{\theta}_D]. \tag{19}$$

The ML estimator of $\boldsymbol{\theta}$ can be derived from the signal model (2) [16]. However, this estimator requires the solution of a $10D$-dimensional maximization problem, which is too complex for implementation in real applications. As an alternative, we resort to a SAGE algorithm [13], [12] as an approximation of the ML estimator. Due to the limitation of space, we will not describe the SAGE algorithm in this contribution.

V. Experimental Investigations

To assess whether the proposed characterization is applicable in real situations, we use the SAGE algorithm to estimate the direction-delay power spectrum (9) of a propagation channel from measurement data collected using the MIMO wideband channel sounder Propsound CS in the measurement campaign described in [17], [18]. We select a measurement conducted in an office, the premises of which are shown in Fig. 2. A description of the measurement setting can be found in [10]. The locations of the Rx and Tx were kept fixed during the measurement. A 50-element omni-directional antenna array was used in the Tx. The Rx was equipped with a single omni-directional antenna. A detailed description of the configuration of the Tx antenna array can be found in [19, Fig. 2]. During the measurement, people were moving in the room where the Tx was located. These movements introduced time variations of the channel response.

The data of 200 measurement cycles were collected within a period of 13 seconds. A measurement cycle is referred to as the interval within which all 50 subchannels are sounded once. Fig. 3 depicts the estimated delay power spectrum calculated from the data.

The SAGE algorithm was used to compute an estimate $\hat{P}(\boldsymbol{\Omega}, \tau)$ of the direction–delay power spectrum $P(\boldsymbol{\Omega}, \tau)$ in (9) within the delay ranging from 100 ns to 135 ns. The estimated number of components $\hat{D}$ is set according to the number of observed dominant local maxima of the direction-delay Bartlett spectrum computed from the measurement data within this delay range: $\hat{D} = 10$. Fig. 4 depicts the 3 dB-spread surfaces (18) of the estimated component azimuth-elevation-delay psds. The color of the surfaces codes the estimated component power.

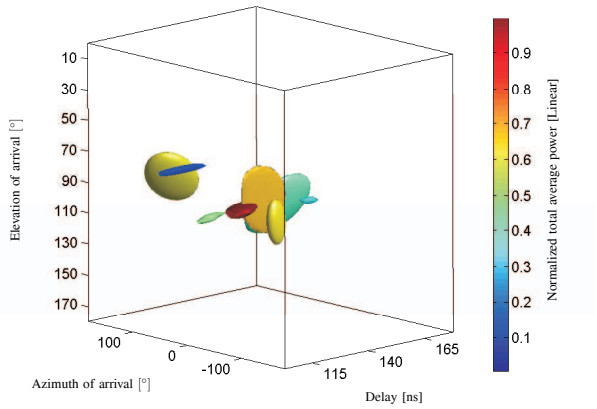

Fig. 4. 3 dB-spread surfaces of estimated component azimuth–elevation–delay power spectra. The color of the surfaces codes the component power estimates.

Fig. 5 depicts the estimated azimuth–elevation–delay power spectrum calculated using the Bartlett beamformer [20] and the azimuth–elevation–delay power spectrum estimate

$$\hat{P}(\phi, \theta, \tau) = \sin(\theta) \cdot \hat{P}(\boldsymbol{\Omega}, \tau)|_{\boldsymbol{\Omega}=\boldsymbol{e}(\phi,\theta)}$$

obtained from the parameter estimates computed with the SAGE algorithm. The notation "$\mathrm{Bartlett}(\boldsymbol{\Sigma})$" in Fig. 5 represents the power spectrum estimate calculated using the Bartlett beamformer applied to the covariance matrix $\boldsymbol{\Sigma}$ given as an argument. For notational brevity, we call such a spectrum "Bartlett spectrum" in the sequel. The matrices $\hat{\boldsymbol{\Sigma}}$ and $\boldsymbol{\Sigma}(\hat{\boldsymbol{\theta}})$ denote respectively the sample covariance matrix and the covariance matrix computed based on $\hat{P}(\boldsymbol{\Omega}, \tau)$.

It is apparent from Fig. 5 that the individual components in $\hat{P}(\phi, \theta, \tau)$ are much more concentrated than the corresponding components in both Bartlett spectra. Furthermore, the symmetry axes of the individual components of $\hat{P}(\phi, \theta, \tau)$ are not parallel to the azimuth and elevation axes. This asymmetry is due to the dependence across different dispersion dimensions. Notice that the Jacobian in (17) can also induce an artificial tilting of the components. However, in this particular example most of the components in $\hat{P}(\phi, \theta, \tau)$ are concentrated in an elevation range around 90°, i.e. over which the impact of the Jacobian is insignificant.

It can be observed from Fig. 5 that the spectra $\mathrm{Bartlett}(\hat{\boldsymbol{\Sigma}})$ and $\mathrm{Bartlett}(\boldsymbol{\Sigma}(\hat{\boldsymbol{\theta}}))$ are similar. However, some of the foot prints arising in $\mathrm{Bartlett}(\hat{\boldsymbol{\Sigma}})$ do not have their counterpart in

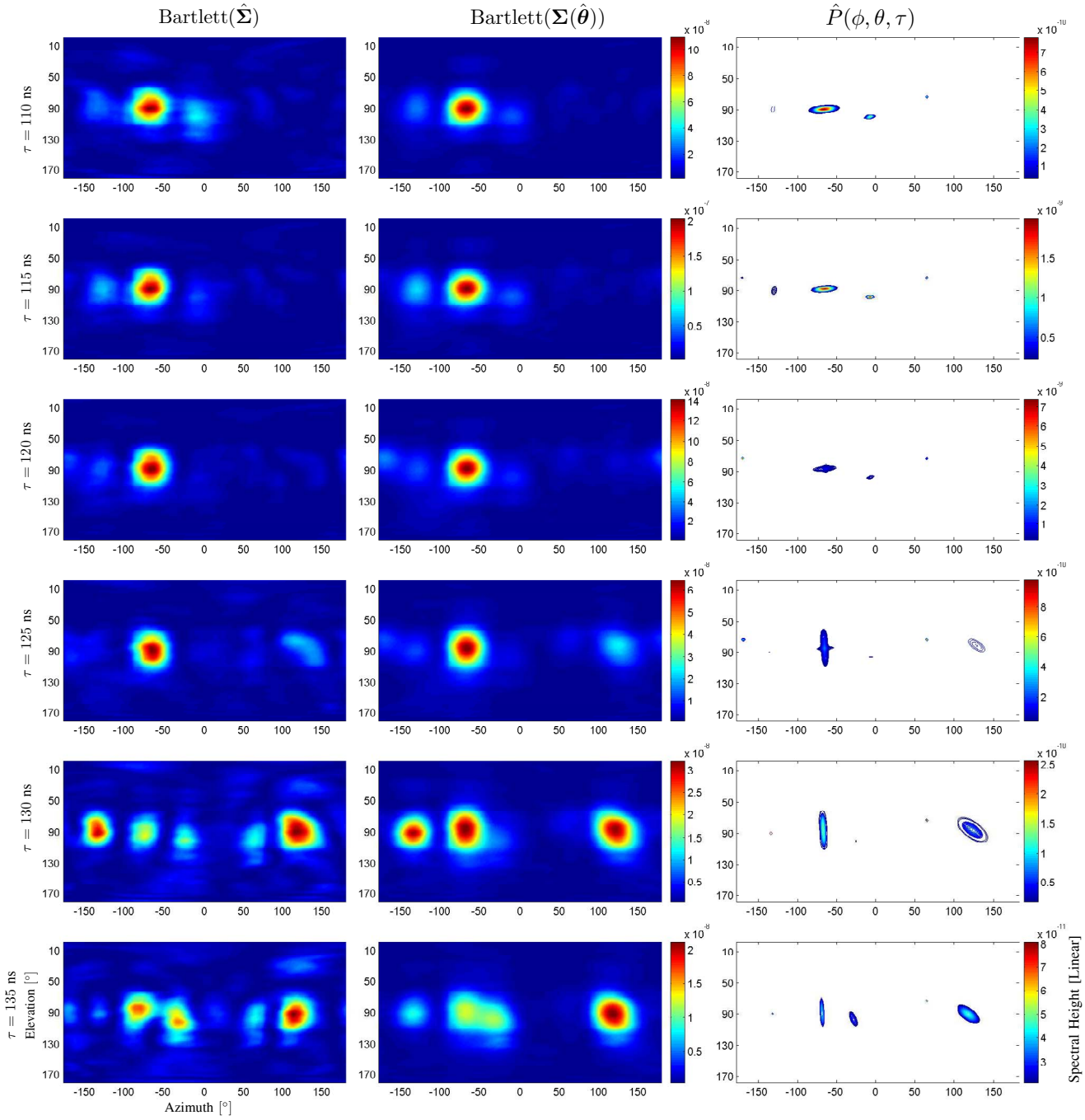

Fig. 5. Bartlett azimuth–elevation–delay spectrum (first two columns) and estimated azimuth–elevation–delay power spectrum computed from the parameter estimates returned by the SAGE algorithm (third column). Each row is plotted for the delay given to its left.

$\mathrm{Bartlett}(\mathbf{\Sigma}(\hat{\boldsymbol{\theta}}))$, which indicates that the number of components $\hat{D}$ specified in the SAGE algorithm is less than the true number of components in the channel response. Furthermore, $\mathrm{Bartlett}(\hat{\mathbf{\Sigma}})$ and $\mathrm{Bartlett}(\mathbf{\Sigma}(\hat{\boldsymbol{\theta}}))$ are slightly different in their significant global and local maxima. A possible explanation for this effect is that the derived pdf (17) only provides an approximation to the effective psd of individual components.

VI. Conclusions

In this contribution, we characterized the normalized direction-delay power spectral density of individual dispersed components in the response of the propagation channel with a probability density function (pdf). The proposed pdf maximizes the entropy under the constraint that its first and second moments are specified. A SAGE algorithm was used to estimate the parameters of the component direction–delay power spectra from measurement data. The results showed that the Bartlett spectra obtained from the reconstructed signal covariance matrix computed using the SAGE estimation result look similar to those calculated using the sample covariance matrix. Furthermore, the estimated component direction-delay power spectra are much more concentrated than their counterpart in the Bartlett spectra. These results demonstrate that the proposed pdf along with the SAGE estimator provide an effective tool to characterize direction-delay dispersion in the propagation channel.

VII. Acknowledgement

This work was jointly supported by the FP7 Network of Excellence in Wireless COMmunications (NEWCOM++) and Elektrobit, Finland.

References

[1] T. Betlehem, T. D. Abhayapala, and T. A. Lamahewa, "Space-time MIMO channel modelling using angular power distributions," in *Proceedings of the 7th Australian Communications Theory Workshop*, Perth, Australia, February, 1-3 2006, pp. 165 – 170.

[2] L. Correia, Ed., *Wireless Flexible Personalised Communications*. John Wiley & Sons, 2001.

[3] J. Medbo, M. Riback, and J. Berg, "Validation of 3GPP spatial channel model including WINNER wideband extension using measurements," in *Proceedings of IEEE 64th Vehicular Technology Conference, (VTC2006-Fall)*, Montréal, Canada, September, 25-28 2006.

[4] N. Czink, X. Yin, H. Özcelik, M. Herdin, E. Bonek, and B. Fleury, "Cluster characteristics in a MIMO indoor propagation environment," *IEEE Transactions on Wireless Communications*, vol. 6, no. 4, pp. 1465–1476, April 2007.

[5] M. Bengtsson and B. Völcker, "On the estimation of azimuth distributions and azimuth spectra," in *Proceedings of the 54th IEEE Vehicular Technology Conference (VTC2001-Fall)*, vol. 3, no. 12, Atlantic City, USA, October 2001, pp. 1612–1615.

[6] T. Trump and B. Ottersten, "Estimation of nominal direction of arrival and angular spread using an array of sensors," *Signal Processing*, vol. 50, pp. 57–69, Apr. 1996.

[7] O. Besson and P. Stoica, "Decoupled estimation of DoA and angular spread for spatially distributed sources," *IEEE Transaction on Signal Processing*, vol. 49, pp. 1872–1882, 1999.

[8] C. B. Ribeiro, E. Ollila, and V. Koivunen, "Stochastic maximum likelihood method for propagation parameter estimation," in *Proceedings of the 15th IEEE International Symposium on Personal, Indoor and Mobile Radio Communications (PIMRC'06)*, vol. 3, Helsinki, Finland, September, 11-14 2004, pp. 1839 – 1843.

[9] E. Jaynes, *Probability theory*. Cambridge University Press, 2003.

[10] X. Yin, T. Pedersen, N. Czink, and B. H. Fleury, "Parametric characterization and estimation of bi-azimuth dispersion of path components," in *Proceedings of the 7th IEEE International Workshop on Signal Processing Advances for Wireless Communications (SPAWC)*, Nice, France, July 2006.

[11] X. Yin, L. Liu, D. Nielsen, N. Czink, and B. H. Fleury, "Characterization of the azimuth-elevation power spectrum of individual path components," in *Proceedings of the International ITG/IEEE Workshop on Smart Antennas (WSA 2007)*, Vienna, Austria, Feb. 2007.

[12] X. Yin, L. Liu, D. Nielsen, T. Pedersen, and B. Fleury, "A SAGE algorithm for the estimation of direction power spectrum of individual path components," in *Proceedings of the 50th IEEE Global Telecommunications Conference (GLOBECOM 2007)*, Washinton D.C. USA, November 2007.

[13] B. H. Fleury, "First- and second-order characterization of direction dispersion and space selectivity in the radio channel," *IEEE Transactions on Information Theory*, no. 6, pp. 2027–2044, Sept. 2000.

[14] K. V. Mardia, "Statistics of directional data," *Journal of the Royal Statistical Society. Series B (Methodological)*, vol. 37, pp. 349–393, 1975.

[15] J. T. Kent, "The Fisher-Bingham distribution on the sphere," *Journal of the Royal Statistical Society, Series B (Methodological)*, vol. 44, pp. 71–80, 1982.

[16] H. Krim and M. Viberg, "Two decades of array signal processing research: the parametric approach," *IEEE Transactions on Signal Processing*, vol. 13, pp. 67–94, 1996.

[17] N. Czink, E. Bonek, X. Yin, and B. H. Fleury, "Cluster angular spreads in a MIMO indoor propagation environment," in *Proceedings of the 16th IEEE International Symposium on Personal, Indoor and Mobile Radio Communications (PIMRC'05)*, vol. 1, Berlin, Germany, September, 11-14 2005, pp. 664–668.

[18] E. Bonek, N. Czink, V. M. Holappa, M. Alatossava, L. Hentilä, J. Nuutinen, and A. Pal, "Indoor MIMO measurements at 2.55 and 5.25 GHz - a comparison of temporal and angular characteristics," in *Proceedings of the 15th IST Mobile Summit*, Myconos, Greece, June, 4-8 2006.

[19] X. Yin, T. Pedersen, N. Czink, and B. H. Fleury, "Parametric characterization and estimation of bi-azimuth and delay dispersion of path components," in *Proceedings of The First European Conference on Antennas and Progation (EuCAP'06)*, Acropolis, Nice, France, November 2006.

[20] M. Bartlett, "Smoothing periodograms from time series with continuous spectra," *Nature*, vol. 161, 1948.